Polar structures in binary mixtures of bent-core liquid crystals showing ferroelectric and antiferroelectric *B*2 phases

Yuya Niigawa,[1] Koushi Nishida,[1] Won Jeon Kim,[2] Seng Kue Lee,[2] Sung Heo,[2] Jong Gun Lee,[2] Fumito Araoka,[1]
Yoichi Takanishi,[1] Ken Ishikawa,[1] Kyung-Tae Kang,[2] Mojca Čepič,[3] and Hideo Takezoe[1]

[1]*Department of Organic and Polymeric Materials, Tokyo Institute of Technology, O-okayama, Meguro-ku, Tokyo 152-8552, Japan*

[2]*Department of Chemistry and Chemistry Institute for Functional Materials, Pusan National University,*

Pusan 609-735, Korea

[3]*Jozef Stefan Institute, Jamova 39, 1000 Ljubljana, Slovenia*

(Received 10 March 2007; published 5 September 2007)

We have studied the polar structures in the binary mixtures of bent-core liquid crystals P-*n*-O-PIMB(n -2)*-($n-4$)O showing the ferroelectric smectic-$C_A P_F$ (Sm-$C_A P_F$) ($n=8$ and 10) and antiferroelectric Sm-$C_S P_A$ ($n=9$) *B*2 phase. Although the polar structure of the one-to-one mixture is governed by the compound with longer end chains, it is much more complicated in the mixtures with slightly less fraction of compounds with longer end chains. Even if the mixtures show the antiferroelectric phase before field application, the ferroelectric domains remain once the field is applied and coexist with the antiferroelectric domains. The coexistence structure was modeled by comparing the microscope real image with that of second-harmonic generation. The fraction of the ferroelectric domains is larger at higher temperature region of the *B*2 phase and decreases with decreasing temperature. The stable phase structures were discussed based on the phenomenological theory. We suggest that the coupling energy of the layer chirality is higher than the energies of the orientation correlations of tilts and polarizations between adjacent layers.

I. INTRODUCTION

The chiral smectic-C^* (Sm-C^*) ferroelectric liquid crystal (FLC) phase was discovered due to an idea of Meyer *et al.* [1]. However, none could predict the antiferroelectric liquid crystal (AFLC) phase [2]. In other words, the FLC and AFLC phases were discovered intentionally and accidentally, respectively. Since then, many researchers tried to understand why the AFLC phase emerges among the same class of mesogenic groups as those showing the FLC phase [3]. Up until now, however, no rational and convincing reasoning on this problem has been made, despite many experimental and theoretical attempts [3–5]. The situation is also the same for bent-core liquid crystals [6], which are the first liquid crystals exhibiting the ferroelectric and antiferroelectric phases without introducing molecular chirality. This problem has been discussed on some homologous series with chiral end chains, as will be described below.

Recently Kumazawa *et al.* [7] and Lee *et al.* [8] found that the chiral analog of the conventional bent-core mesogens P-*n*-O-PIMB($n-2$)* and P-*n*-O-PIMB($n-2$)*-($n-4$)O exhibit the odd-even behavior for the emergence of ferroelectric (F, even *n*) and antiferroelectric (AF, odd *n*) *B*2 phases. Nishida *et al.* [9] discussed the odd-even effect based on a simple phenomenological theory including the interaction energies of van der Waals, dipolar and steric in origin, and proposed an interpretation. In order to understand the interaction of end chains in adjacent layers, Nishida *et al.* [10] also studied the phase behavior of the asymmetric bent-core mesogens with odd and even carbon numbers in their end chains and the one-to-one mixtures of these compounds with even and odd *n*. They found that mesogens with longer chain length play a dominant part for the phase structure. However, they used only one-to-one mixtures. To understand

more delicate balance between ferroelectricity and antiferroelectricity in the mixture systems, full studies using mixtures of varying ratios are necessary. Such study was made by Nakata *et al.* [11] using mixtures of P-8-OPIMB6* and P-8-O-PIMB. Although two-component compounds have different types of end chains, chiral and nonchiral, interesting competition behavior between ferroelectricity and antiferroelectricity was obtained. In the 4:6 mixture, a ferroelectric to antiferroelectric state change occurs with decreasing temperature. In this paper, we study the phase behavior of binary mixtures of neighboring homologues exhibiting ferroelectric and antiferroelectric phases: i.e., P-8-O-PIMB6*-4O/P-9-O-PIMB7*5O (P8/P9) and P-9-O-PIMB7*-5O/P-10-O-PIMB8*-6O (P9/P10) by means of texture observations, second harmonic generation (SHG) measurements and SHG microscopy. The results were discussed based on a simple phenomenological theory. The microscopic origin of interactions and their temperature and mixing ratio dependence are considered. The coexistence of the AF and F domains can be described by a higher-order term in the free energy which favors antichiral (racemic) interlayer ordering.

II. EXPERIMENT

The samples used were two series of mixtures of P-*n*-O-PIMB($n-2$)*-($n-4$)O (Fig. 1) [8]: namely, P-8-O-PIMB6*-4O/P-9-O-PIMB7*-5O (P8/P9) and P-9-O-PIMB7*-5O/P-10-O-PIMB8*-6O (P9/P10) with various mixing ratios. Two compounds were dissolved in chloroform solution, and the mixtures were obtained by evaporating the chloroform. The sample was introduced into sandwich-type cells using two indium-tin-oxide-coated glass
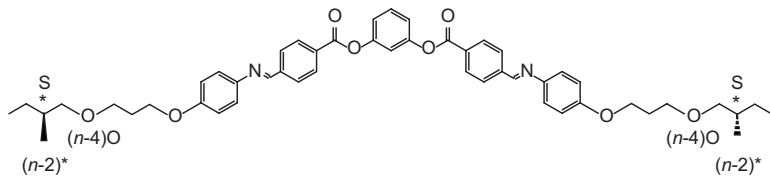
plates. Neither polymer coating nor rubbing was made on the substrate surfaces.

To investigate the polar structure, a macroscopic and a microscopic observation of the SHG were carried out. The former was based on the conventional system using a *Q*-switched Nd:YAG laser (10 Hz, 1064 nm) as a fundamental light source. In this case, an SH light generated by an oblique incident beam was detected by a photomultiplier tube (PMT) settled in the transmission direction with neither focusing nor collecting lens. The viewing area is much larger than the domain size and is about 1 mm after passing through an aperture, so that the signal is averaged one over randomly oriented ferroelectric and antiferroelectric domains. The latter utilized a highly sensitive cooled charge-coupled device (CCD) instead of a PMT. To obtain the SH signal as an image, a 20× objective and a 200-mm telephoto lens were introduced to collect the visible light from the sample (Fig. 2). As well, this system enables us to take a real image on the same viewing area as that of the SH image, with a white light source (halogen lamp) instead of the laser.

III. EXPERIMENTAL RESULTS

We focus on the *B*2 phase, which exhibits ferroelectric and antiferroelectric switching. In the *B*2 phase there are four possible states in view of correlations of polar order and molecular tilt direction in successive layers. They are named Sm-$C_{S,A}P_{F,A}$ [12,13], where subscripts *S* and $A-C$ stand for synclinic and anticlinic order between adjacent layers and *F* and $A-P$ stand for the ferroelectric and antiferroelectric organization of polarizations. The tilt direction is not correlated to polar order, unlike rodlike molecules, so the antichiral (racemic) layer structure can exist: i.e., Sm-$C_S P_A$ and Sm-$C_A P_F$.

First we conducted a texture observation in the *B*2 phase with and without applying an electric field in P8/P9 mixtures. Figures 3(a)–3(c) show photomicrographs under crossed polarizers. In a P9-40% mixture, extinction direc-

tions parallel and perpendicular to the polarizers did not change with field application and termination, as shown in Fig. 3(a), suggesting the Sm-$C_A P_F$ state. In a P9-52% mixture, stripes characteristic to the Sm-$C_S P_A$ state were observed in the absence of a field, as shown in Fig. 3(c), left. The stripes vanished by applying a field larger than the threshold field, as shown in Fig. 3(c), right. In our previous paper [8], we reported the odd-even behavior in the emergence of the F and AF phases. According to the rule, P8 and P9 exhibit the F and AF phases, respectively. We pointed out a further rule: the emergence of the phase in a one-to-one mixture of these homologues is governed by the homologue with longer chains [10]. Thus, the present result is in accordance with these rules; these mixtures show the same behavior as that by the dominant components of the mixture: i.e., P8 in P9-40% and P9 in P9-52%.

According to the rule, P9-50% is expected to give the AF phase, the same as P9-52% shown in Fig. 3(c). To see the intermediate mixture behavior between P9-52% and P9-40%, the behavior in P9-45% was examined. As shown in Fig. 3(b), stripes similar to Fig. 3(c) were observed in circular domains before applying a field and were attributed to the
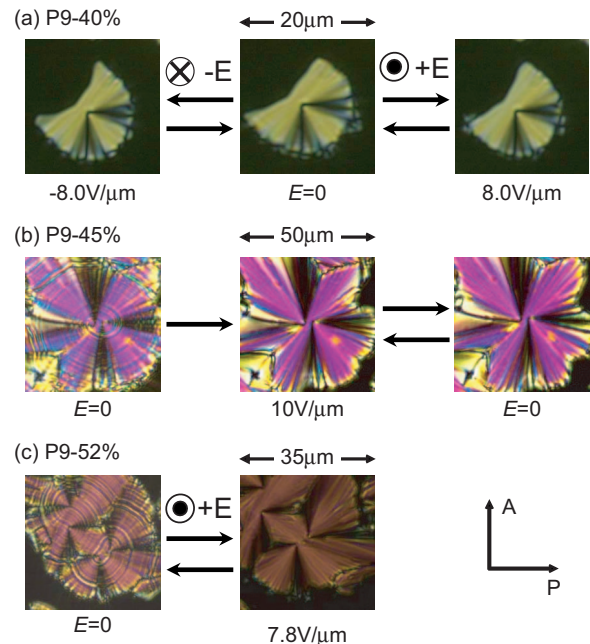
FIG. 3. (Color online) Photomicrographs with and without the field in the *B*2 phase of (a) P9-40%, (b) P9-45%, and (c) P9-52% of P8/P9 mixtures. In P9-40% (a), extinction direction does not change by field application and termination, suggesting Sm-$C_A P_F$. In P9-45% (b), stripes are observed before the field application and disappear by applying the field. But the stripes do not reappear by field termination. In P9-52% (c), stripes are also observed in the absence of a field and disappear in the presence of a field.
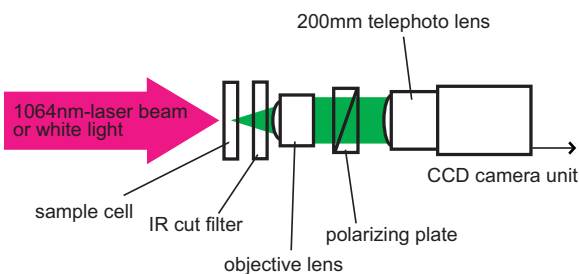

FIG. 2. (Color online) Optical scheme of SH microscopy. An SH light generated from a sample by an incident fundamental beam was detected by a charge-coupled device.
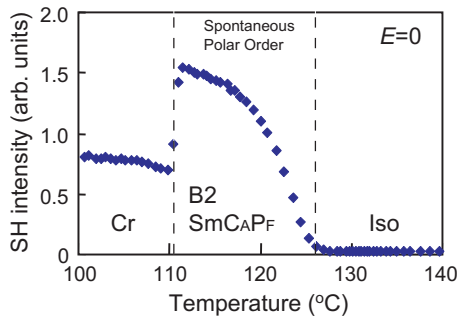
FIG. 4. (Color online) Temperature dependence of SH intensity in P9-40% mixture of P8/P9 in the absence of an electric field. Spontaneous SHG activity indicates the ferroelectric phase.

characteristics in the Sm-$C_S P_A$ state. The electric-field application gave the texture change, as shown in Fig. 3(b). Because of the disappearance of the stripes and the extinction directions parallel to the cross polarizers, the induced state is identified as the Sm-$C_A P_F$ state. A different behavior to P9-52% was observed when the field was turned off: namely, the Sm-$C_A P_F$ state did not relaxed to the original state, Sm-$C_S P_A$, but stayed in Sm-$C_A P_F$. In this way, in the mixtures with nearly equal mixing ratio, competing interactions to realize the F and AF phases give complicated phase behavior.

To further examine the phase behavior in the same mixing ratio range, SHG measurements were performed. First, to convince the spontaneous polar order in P9-40%, the temperature dependence of SH intensity was measured. As shown in Fig. 4, the $B2$ phase is SHG active, indicating ferroelectricity. By contrast, in the antiferroelectric $B2$ state of P9-52% and P9-45%, SH activity is observed only under an electric field. Figures 5(a) and 5(b) are the field dependence of SH intensity in the P9-52% and P9-45% mixtures, respectively. Each measurement was conducted before applying a field in advance after heating the sample to the isotropic phase. In the P9-52% mixture, SH intensity sharply increased above a threshold field at about 1.5 V/μm and saturated at about 2.2 V/μm with increasing the field. In the field-decreasing process, the SH intensity became weaker and finally SH activity almost diminished at zero field, although remnant SHG was observed. The behavior is characteristic to a usual antiferroelectric phase. By contrast, the field dependence of the SH intensity in the P9-45% mixture is interesting, as shown in Fig. 5(b). The SH intensity growth by applying a field to a virgin sample is more or less the same as that in P9-52%. In the field-decreasing process, however, relatively large SH intensity remained even after the field termination, suggesting that only parts of the F domains returned to the AF states upon the field removal. Similar results of the texture observations and the SHG measurements as those in the P8/P9 mixtures were also obtained in the P9/P10 mixtures.

Let us call the $B2x$ region when the mixture exhibits the Sm-$C_S P_A$ phase in virgin cells and the Sm-$C_A P_F$ phase remains once an electric field is applied. This condition appears in the mixture whose mixing ratio is close to 1:1. The fraction of the remnant Sm-$C_A P_F$ domain in the $B2x$ region changes with temperature and is plotted in Fig. 5(c) as rem-
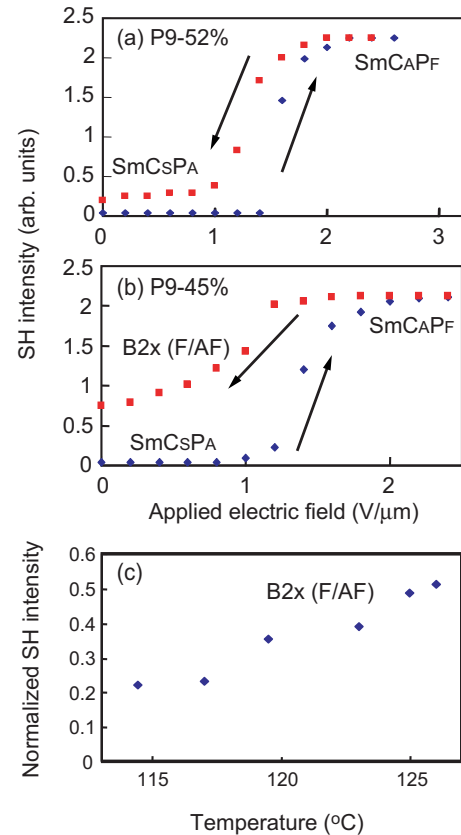

FIG. 5. (Color online) (a) SH intensity with increasing (blue diamonds) and decreasing (red squares) field in a P9-52% mixture. (b) SH intensity with increasing (blue diamonds) and decreasing (red squares) field in a P9-45% mixture. Remnant SH signal at 0 V is seen particularly in a P9-45% mixture. (c) Temperature dependence of the remnant SH intensity in the $B2x$ region of a P8/P9 mixture. The value of the vertical axis is normalized by the SH intensity under a sufficient field.

nant SH intensity: i.e., the SH intensity after decreasing E to zero in Figs. 5(a) and 5(b). The vertical axis (normalized SH intensity) stands for the SH intensity normalized by that under the field to realize fully F domains after gradually decreasing the field to zero. The remnant SHG decreases with decreasing temperature, indicating that the AF phase becomes more stable in lower temperatures. This tendency is the same as that observed previously [11]. It is noted, however, that a virgin sample shows AF domain, as noticed by Fig. 5(b), whereas spontaneous variation from F to AF with decreasing temperature was suggested by the temperature dependence of the dielectric constant in our previous mixture [11]. Once the mixed condition of the F and AF domains is established, the fraction of these domains is quite stable; i.e., the SH intensity was kept constant at least 1 h. Hence, the field-induced F domain is quite stable once it remains upon field termination. The fraction of remnant F domain depends on the field termination procedure; namely, the fraction is larger when the field is suddenly terminated than that when the field is gradually decreased to zero.

The above experimental results indicate that the F and AF domains coexist in the $B2x$ region after terminating the field. Only from the texture observation in the $B2x$ region, how-
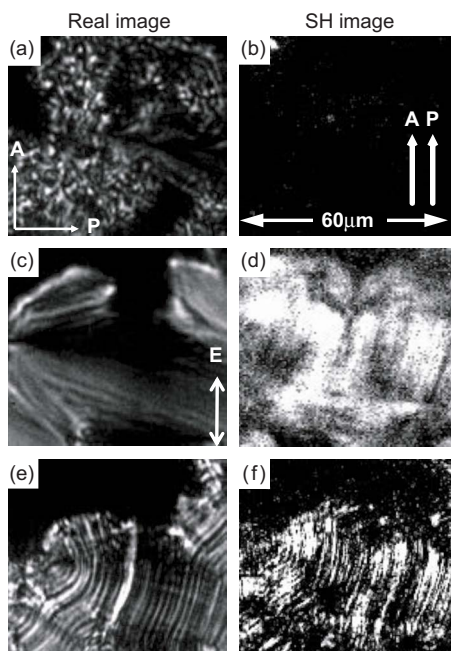
FIG. 6. The microscope real (left row) and SH (right row) images of the $B2x$ region. The field direction is parallel to one of the polarizers as indicated in (c). (a) and (b) before field application, (c) and (d) under 8 V/μm, and (e) and (f) after field termination.

FIG. 7. (Color online) Model structure of the molecular orientations in the $B2x$ region after terminating the field. The regions of Sm-$C_A P_F$ and Sm-$C_S P_A$ are separated by red lines.

ever, it is hard to discuss how the mixed state is: namely, whether simple mixing of Sm-$C_S P_A$ and Sm-$C_A P_F$ or the emergence of other mixed-state-like ferrielectric states [14]. To investigate this problem, second-harmonic generation (SHG) microscopy was carried out in the $B2x$ region of the P8/P9 mixture. In this observation, a cell having in-plane electrodes with a gap of 50 μm was used so that a field direction was parallel to the glass plate. Figure 6 shows real (left row) and SH (right row) images of the domains. Here the polarizers are in the crossed position in the real images and are parallel positions in the SHG images, as shown by white arrows. Figures 6(a) and 6(b), respectively, show real and SH images before applying the field. The SH image is almost completely dark, being consistent with the AF state. By applying an electric field parallel to the analyzer direction [white arrow in (c)], the field-induced F state emerges, which is realized by the real image observation (c) and the SHG activity shown by white region in (d). The real and SHG images after the field termination are shown in Figs. 6(e) and 6(f), respectively. The real image changes from a smooth texture to fringe patterns. The fringe in Fig. 6(e) may represent the boundary between Sm-$C_A P_F$ and Sm-$C_S P_A$. This is because the domain in Fig. 6(e) is partially SHG active, as shown in Fig. 6(f). Some parts of the bright domains in Fig. 6(d) became dark and some emerge as stripes. It is noted that the stripes in the real image [Fig. 6(e)] and the SHG image [Fig. 6(f)] are not necessarily the same, as was noticed by carefully comparing two images.

Based on the SHG microscopy shown in Figs. 6, we discuss the structural model after terminating the field in the $B2x$ region. The structural model should be consistent to the experimental fact that coexisting two domains have the op-
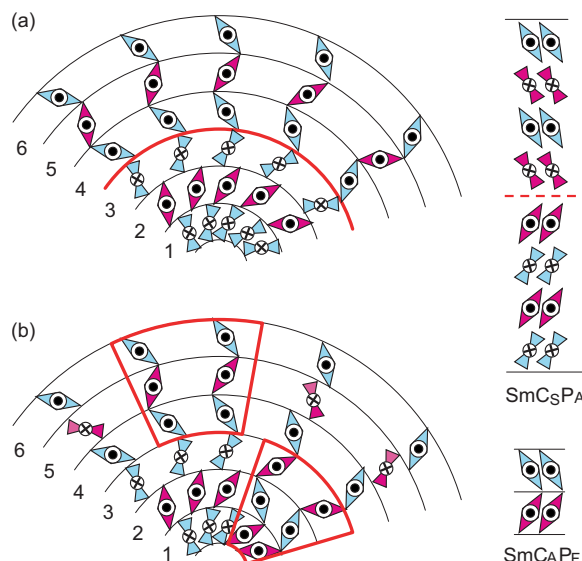
posite polarity and the layer chirality is always racemic: i.e., Sm-$C_A P_F$ and Sm-$C_S P_A$. Two types of coexistence are possible, as shown in Fig. 7. The two fundamental structures Sm-$C_S P_A$ and Sm-$C_A P_F$ are shown on the right-hand side. In the model (a), Sm-$C_S P_A$ and Sm-$C_A P_F$ correspond to layers 1–3 and layers 4–6, respectively, bordered by a red line. The model (b) is much involved. In both layers 1–3 and layers 4–6, two domains coexist. In layers 1 and 3, both chirality and polarity change within each layer, while tilt does not change. In layer 2, both chirality and tilt change within each layer, while polarity does not change. In layer 5, polarity and tilt change within each layer, leaving chirality unchanged, although layers 4 and 6 are uniform. The F domains indicated by red boxes changes to the AF domains along the layer direction. Careful observation of Fig. 6(f) shows there are both cases of models (a) and (b), since changes between white and black occur along the directions both parallel and perpendicular to the layer. In any event, we can conclude that the coexistence occurs macroscopically.

Based on these experimental results, the overall phase diagram in the two series of mixtures P8/P9 and P9/P10 is drawn in Fig. 8. According to the odd-even rule mentioned earlier, the F phase emerges in wide ranges near P8 and P10 and the AF phase in a wide range near P9. In the range close to the 1:1 mixtures, coexistence of two domains of Sm-$C_S P_A$ and Sm-$C_A P_F$ occurs. The phase boundaries are slightly shifted toward the left side, according to the rule established experimentally; namely, the phase behavior in Pn/Pm is governed by Pn ($n > m$). The phase boundaries between Sm-$C_A P_F$ and the $B2x$ region exist between P9-40% and 45% in the P8/P9 mixture and between P9-50% and 55% in the P9/P10 mixture. Those between Sm-$C_S P_A$ and $B2x$ phase exist between P9-50% and 55% in the P8/P9 mixture and between 55% and 60% in the P9/P10 mixture. In the $B2x$ region, the fraction of Sm-$C_A P_F$ is always larger at higher temperatures, whereas Sm-$C_S P_A$ becomes dominant at lower
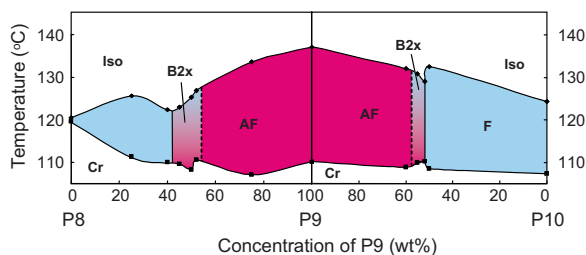
FIG. 8. (Color online) The phase diagram of the two mixtures P8/P9 and P9/P10. The $B2x$ region exists between F and AF phases, in which the field-induced F phase remains after the terminating the field.

temperatures. This behavior is identical to the results reported previously [11].

IV. THEORETICAL

In order to consider stable phase structures realized in the mixtures mentioned above, we now describe the free energy for the bent-core mesogenic system as follows:

$$G_{int} = \sum_j \frac{1}{2} a_{0p} P_j^2 + \frac{1}{4} b_{0p} P_j^4 + \frac{1}{4} c_{0p} P_j^6 + \frac{1}{2} a_{0t} \xi_j^2 + \frac{1}{4} b_{0t} \xi_j^4$$
$$+ \frac{1}{2} \Omega_0 (\vec{\xi}_j \times \vec{P}_j)^2 + \frac{1}{2} a_{1p} (\vec{P}_j \cdot \vec{P}_{j+1}) + \frac{1}{2} a_{1t} (\vec{\xi}_j \cdot \vec{\xi}_{j+1}),$$

(1)

where $\mathbf{P}_j$ and ξ_j are polarization and tilt order parameters for the jth smectic layer, respectively. We limit ourselves to a study of tilt and polarization orientations, and we do not consider the temperature dependence of the nematic and smectic orders, which affect the interlayer interactions. We assume that both of them increase upon decreasing temperature. The subscripts 0 and 1 stand for intralayer and interlayer interactions, respectively. The subscripts p and t are for the interactions expressed by polarization and tilt, respectively. The first three terms give the polarization order contribution to the free energy. The terms are considered up to the sixth order as the described systems become polarly ordered by the strongly discontinuous transition. Similarly, the next two terms give the free energy contribution expressed in tilt order. The term Ω_0 gives the coupling of the tilt and polarization, and the negative sign of this term favors perpendicularity of the tilt and polarization due to the steric constraints. The last two terms give interactions of polarizations and tilts between adjacent layers, respectively.

Our attempt is to consider the relative orientation of tilts (clinicity) and polarizations (polarity) in neighboring layers. Therefore in the free energy we consider only terms that depend on the relative orientations of the polarization and tilt order parameters, the terms with coefficients a_{1p} and a_{1t}. The origin of both coefficients was discussed in our previous paper [9]. The coefficient a_{1p} gives the interaction between polarizations in adjacent layers. It favors ferroelectric ordering of polarizations for its negative sign and the antiferroelectric ordering for its positive sign of the coefficient. There

are three contributions of different microscopic origin to this coefficient:

$$a_{1p} = a_{1p,VW} + a_{1p,D} + a_{1p,S}. \tag{2}$$

The $a_{1p,VW}$ gives the van der Waals attractive interaction. It favors ferroelectric ordering, as parts of the positionally correlated molecules in neighboring layers, which only contribute to interlayer interactions, are less distant than in the antiferroelectric ordering [9]. Therefore the contribution has a negative sign. The next contribution to the a_{1p} is given by electrostatic interactions between molecular dipoles, $a_{1p,D}$. This interaction also exists only when positional correlations are present and favors antiferroelectric ordering [15]. The contribution is positive. The last contribution to the a_{1p} arises due to the steric interaction $a_{1p,S}$: i.e., partial penetration of molecular tails to neighboring layers and the consequent favorable parallel orientations of branches. The contribution is positive as parallel braches require antiferroelectric polarizations.

The significance of these contributions is strongly influenced by molecular positional correlations [16]. If for molecules in neighboring layers positional correlations do not exist, i.e., the smectic layer can be considered as an ideal liquid. In this occasion, van der Waals attraction keeps layers sticking together, but does not influence their orientation. Positional correlations of molecules in neighboring layers decrease with increasing smectic order, as molecules less interpenetrate to neighboring layers and layers can therefore glide as a whole. The smectic order can increase due to various reasons. For the system studied two effects are important. First, the molecular structure and the orientation of the chiral groups which can prohibit or stimulate the interlayer penetration of molecular branches and consequently influences smectic order. This explains the odd-even behavior in two homologous series of the chiral analogs of Pn-O-PIMB [9]. Second, the temperature variations which increase the smectic order upon lowering the temperature due to the decrease of entropy. In both cases we can expect that all the contributions $a_{1p,VW}$, $a_{1p,D}$, and $a_{1p,S}$ decrease with temperature, because the smectic order increases.

The second term a_{1t} gives interlayer interactions that are influenced by the tilt. Two types of microscopic contributions have to be considered, the van der Waals attraction $a_{1t,VW}$ and the contribution due to the steric repelling interactions which arise due to the partial interpenetration of the molecular tails to neighboring layers $a_{1t,S}$:

$$a_{1t} = a_{1t,VW} + a_{1t,S}. \tag{3}$$

The van der Waals attraction $a_{1t,VW}$ favors anticlinic tilts and contributes positively to the coefficient a_{1t}. The steric interaction favors synclinic order in neighboring layers and contributes negatively to the a_{1t}. Both interactions decrease with increasing smectic order.

Mixing experiments and the phase diagram experimentally obtained offer additional information about the relative strengths of quoted contributions, their temperature dependences, and the nature of the interlayer interactions with respect to their origins in general. The interlayer interactions change with temperature and concentration (mixing ratio). In

order to understand the behavior qualitatively we assume a simple linear dependence on temperature originating in increasing smectic order of the two coefficients,

$$a_{1p} = a_{1p0}[T - T_p(c)],$$

$$a_{1t} = a_{1t0}[T - T_t(c)]. \tag{4}$$

Here c, T_p, and T_t are the concentration and the temperatures, where a_{1p} and a_{1t} change the sign; i.e., correlations of polarity and clinicity change, respectively. Both temperatures depend on concentration c. Coefficients a_{1p0} and a_{1t0} are reference values. One cannot expect that both temperatures are the same, since these interactions have different origins. Therefore one could expect the phase change between Sm-$C_A P_F$ and Sm-$C_S P_A$ via either Sm-$C_A P_A$ or Sm-$C_S P_F$—i.e., Sm-$C_A P_F \leftrightarrow$ Sm-$C_A P_A \leftrightarrow$ Sm-$C_S P_A$ or Sm-$C_A P_F \leftrightarrow$ Sm-$C_S P_F \leftrightarrow$ Sm-$C_S P_A$—depending which temperature, T_p or T_t, is higher.

Experimental results clearly show that, in the intermediate region, domains of Sm-$C_A P_F$ and Sm-$C_S P_A$ exist simultaneously. The SHG results indicate that at higher temperature ferroelectric domains are more favorable and at lower temperature the system favors antiferroelectric domains. These facts define the signs of reference coefficients—i.e., a_{1p0} is negative and a_{1t0} is positive—to describe the system correctly. From this behavior one can conclude that interactions originated from van der Waals interactions ($a_{1p,VW}$ and $a_{1t,VW}$) decrease faster upon lowering the temperature than the interactions of steric origin ($a_{1p,S}$ and $a_{1t,S}$). Because van der Waals interactions strongly depend on positional correlations between molecules in neighboring layers, they are more strongly affected by the increase of the smectic order than interpenetration of molecular branches and consequent transfer of the branch direction from layer to layer. The reasoning is consistent with experimental observations.

Next, experiments indicate no sign of the stepwise phase transitions, where first changes clinicity and later polarity or vice versa. The intermediate phase should be structurally homochiral as both phases in pure systems are antichiral (racemic). It seems that the change of the layer chirality is strongly disfavored. Therefore an additional higher-order term, which describes the coupling of the layer chirality, has to be added to the free energy [17] to account for the observed behavior:

$$+ \frac{1}{2}\Omega_1[(\vec{\xi}_j \times \vec{P}_j) \cdot (\vec{\xi}_{j+1} \times \vec{P}_{j+1})]. \tag{5}$$

The coefficient Ω_1 is positive as it favors opposite signs of structural chirality given by $(\vec{\xi}_j \times \vec{P}_j)$ in the jth smectic layer. The structural chirality describes the mutual tilt polarization orientation in the layer, can have two opposite signs, and is not related to or influenced by the molecular chirality in bent-core systems. Such a term can also be explained from the microscopic origin. It favors both (i) parallelism of the bent molecules branches in neighboring layers for the Sm-$C_S P_A$ structure favored by molecular partial interpenetrations and (ii) the shortest distances between parts of the molecules in neighboring layers for the Sm-$C_A P_F$ favored by

attractive van der Waals interactions. Such interactions lead to the nonexistence of the intermediate homochiral states. Experimental results enable us to set the limits on the coefficient relations. The antichiral (racemic) states are stable as long as

$$\left| \frac{1}{2}\Omega_1 \theta^2 P^2 \right| > \left| \frac{1}{2}a_{1p}P^2 \right| \quad \text{or} \quad \left| \frac{1}{2}\Omega_1 \theta^2 P^2 \right| > \left| \frac{1}{2}a_{1t}\theta^2 \right|. \tag{6}$$

As soon as both coefficients a_{1p} and a_{1t} change sign, the competition is lost and domains of the other antichiral structure become likely. It is most likely that during the transition the molecules rotate on the cone and the chiral structure is preserved. The energy barrier appears due to the unfavorable states during the rotation and is penalized either by

$$|a_{1p}P^2| \quad \text{or} \quad |a_{1t}\theta^2|, \tag{7}$$

depending on which coefficient a_{1p} or a_{1t} has unfavorable sign. In this way, the higher-order term, which describes the coupling of the layer chirality, plays an important role in the coexistence of Sm-$C_S P_A$ and Sm-$C_A P_F$ and in the field-induced and temperature-induced transition from Sm-$C_S P_A$ to Sm-$C_A P_F$.

The described reasoning can also explain similar observations reported by Umadevi *et al.* [18]. As achiral bent-core molecules also show an odd-even effect, the promotion or prevention of partial diffusion appears due to the structure of terminal chains. The structure is affected by the number of constituents in the terminal chains, and tails become more flexible with increasing length, giving rise to a fading of the effect.

V. CONCLUSIONS

Binary mixtures of P-8-O-PIMB6*-4O/P-9-O-PIMB7*-5O (P8/P9) and P-9-O-PIMB7*-5O/P-10-O-PIMB8*-6O (P9/P10) were investigated by means of texture observations, SHG measurements, and SHG microscopy. When the proportion of one compound is much higher than the other, the characteristics of the major compound are dominant. On the other hand, when the mixing ratio is close to 1:1, interesting textures are observed. In this case, synclinic AF domains in the ground state switch into field-induced anticlinic F domains. But unlike in the case of the usual AF states, parts of the domains stay in the F states after field termination. F and AF states coexist in each domain of this state. In other words, different senses of polarity coexist in the racemic domains. The stable phase structures were discussed based on consideration of the microscopic origins of the terms in the phenomenological theory. The importance of the higher-order coupling term of the layer chirality was suggested.

[1] R. B. Meyer, L. Liebert, L. Strzelecki, and P. Keller, J. Phys. (Paris) **36**, L69 (1975).

[2] A. D. L. Chandani, E. Gorecka, Y. Ouchi, H. Takezoe, and A. Fukuda, Jpn. J. Appl. Phys., Part 2 **28**, L1265 (1989).

[3] A. Fukuda, Y. Takanishi, T. Isozaki, K. Ishikawa, and H. Takezoe, J. Mater. Chem. **4**, 997 (1994).

[4] J. Thisayukta and E. T. Samulski, J. Mater. Chem. **14**, 1554 (2004).

[5] M. A. Glaser and N. A. Clark, Phys. Rev. E **66**, 021711 (2002).

[6] T. Niori, T. Sekine, J. Watanabe, T. Furukawa, and H. Takezoe, J. Mater. Chem. **6**, 1231 (1996).

[7] K. Kumazawa, M. Nakata, F. Araoka, Y. Takanishi, K. Ishikawa, J. Watanabe, and H. Takezoe, J. Mater. Chem. **14**, 157 (2004).

[8] S. K. Lee, S. Heo, J. G. Lee, K.-T. Kang, K. Kumazawa, K. Nishida, Y. Shimbo, Y. Takanishi, J. Watanabe, T. Doi, T. Takahashi, and H. Takezoe, J. Am. Chem. Soc. **127**, 11085 (2005).

[9] K. Nishida, M. Čepič, W. J. Kim, S. K. Lee, S. Heo, J. G. Lee, Y. Takanishi, K. Ishikawa, K.-T. Kang, J. Watanabe, and H. Takezoe, Phys. Rev. E **74**, 021704 (2006).

[10] K. Nishida, W. J. Kim, S. K. Lee, S. Heo, J. G. Lee, K.-T. Kang, Y. Takanishi, K. Ishikawa, J. Watanabe, and H. Takezoe, Jpn. J. Appl. Phys., Part 2 **45**, L1246 (2006).

[11] M. Nakata, D. R. Link, J. Thisayukta, Y. Takanishi, K. Ishikawa, J. Watanabe, and H. Takezoe, J. Mater. Chem. **11**, 2694 (2001).

[12] D. M. Walba, E. Korblova, R. Shao, J. E. Maclennan, D. R. Link, M. A. Glaser, and N. A. Clark, Science **288**, 2181 (2000).

[13] H. Takezoe and Y. Takanishi, Jpn. J. Appl. Phys., Part 1 **45**, 597 (2006).

[14] M. Zennyoji, Y. Takanishi, K. Ishikawa, J. Thisayukta, J. Watanabe, and H. Takezoe, J. Mater. Chem. **9**, 2775 (1999).

[15] M. Čepič, B. Žekš, and J. Mavri, Mol. Cryst. Liq. Cryst. Sci. Technol., Sect. A **328**, 47 (1999); and M. Čepič and B. Žekš, *ibid.* **301**, 221 (1997).

[16] R. Bruinsma and J. Prost, J. Phys. II **4**, 1209 (1994).

[17] J. V. Selinger, Phys. Rev. Lett. **90**, 165501 (2003).

[18] S. Umadevi, A. Jakli, and B. K. Sadashiva, Soft Matter **2**, 857 (2006).